

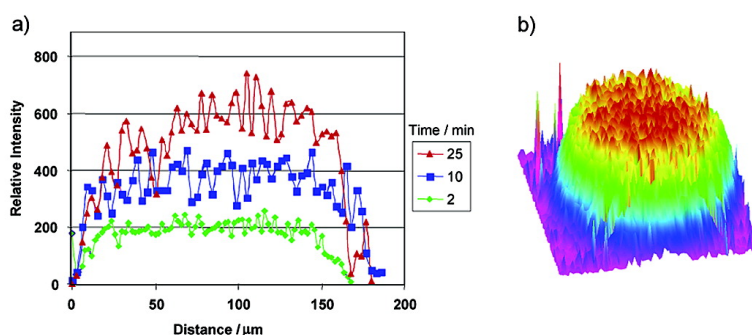
Article

Which Sites React First? Functional Site Distribution and Kinetics on Solid Supports Investigated Using Confocal Raman and Fluorescence Microscopy

Jrgen Kress, Riccardo Zanaletti, Abigail Rose, Jeremy G. Frey, William S. Brocklesby, Mark Ladlow, and Mark Bradley

J. Comb. Chem., **2003**, 5 (1), 28-32 • DOI: 10.1021/cc020024x • Publication Date (Web): 17 December 2002

Downloaded from <http://pubs.acs.org> on March 20, 2009



More About This Article

Additional resources and features associated with this article are available within the HTML version:

- Supporting Information
- Links to the 3 articles that cite this article, as of the time of this article download
- Access to high resolution figures
- Links to articles and content related to this article
- Copyright permission to reproduce figures and/or text from this article

[View the Full Text HTML](#)

Which Sites React First? Functional Site Distribution and Kinetics on Solid Supports Investigated Using Confocal Raman and Fluorescence Microscopy

Jürgen Kress,[†] Riccardo Zanaletti,[†] Abigail Rose,[†] Jeremy G. Frey,[†]
William S. Brocklesby,[‡] Mark Ladlow,[§] and Mark Bradley^{*,†}

*Department of Chemistry, University of Southampton, Southampton SO17 1BJ, United Kingdom,
Department of Physics and the Opto-Electronics Research Centre, University of Southampton,
Southampton SO17 1BJ, United Kingdom, GlaxoSmithKline, Chemistry Technologies, Department of
Chemistry, University of Cambridge, Lensfield Road, Cambridge CB2 1E, United Kingdom*

Received April 3, 2002

Fluorescence microscopy is a powerful technique for analyzing beads with very low loadings of fluorophores; however, the method is flawed when looking at more highly loaded beads as a result of severe problems with absorption. To probe distributions at higher loading levels, Raman spectroscopy avoids many of these issues. These studies show that there is a uniform distribution of reactive sites throughout the beads but that the spatial distribution of reacted sites depends on the polymer type, with a fine balance between reaction and diffusion rate.

Resin beads are used in a large number of chemical and biological processes ranging from synthesis¹ to screening, where beads have been used, for example, in scintillation proximity assays,² as supports for fluorescent sensors,³ and as screening vehicles.⁴ However, for resin beads to be more fully exploited, especially in the area of bead screening and sensors, it is important to obtain a more detailed understanding of the solid supports with respect to the diffusion of reagents into the beads and the distribution of the functional sites within the supports. Methods that have been used to probe bead functionality include autoradiography,⁵ scanning secondary ion mass spectrometry,⁶ and confocal microscopy.^{7,8} However, in the area of fluorescence, it is important to understand the interactions and complexities that take place within beads during investigation, and although some papers have been published in this area, there is still much confusion.^{8–10} Here, we wish to report our findings on the site distribution found within PS, TentaGel, and controlled pore glass (CPG) beads using confocal fluorescence microscopy and to show how Raman spectroscopy can solve some of the inherent problems associated with the latter technique.

Confocal microscopy allows fluorescence spectra to be recorded from a volume element of $\sim 1 \times 1 \times 3 \mu\text{m}^{11,12}$ from anywhere within the bead (Figure 1), while spectra can be collected in a consecutive fashion, for example, by scanning along a line or across a plane. The amino-functionalized solid supports TentaGel, PEGA, and beaded controlled pore glass (CPG) were first loaded with rhodamine isothiocyanate (RITC) in order to “tag” the functional groups.

Since it was known that fluorescence spectra taken from beads have to be treated with some care,^{7,8} the loading of the beads with RITC was chosen to be rather low for two reasons. First, high levels of fluorophore prevent light from entering more than a few micrometers into the bead (Figure 1b); second, high levels of fluorophore also lead to significant reabsorption of the fluorescence (for even low Stokes shifts, there is still sufficient overlap between the emission and absorption bands of fluorescent dyes). The result is that absorption of both excitation and fluorescent radiation will be much more significant for fluorescence at the center of the bead, since the light has a longer way to travel both into and out of the bead than light from the bead edges (Figure 1a). These two scenarios result in a lower fluorescence output from the center of the bead than the edge, although the loading is constant (see Figure 2).

The absorbance issues can be explained in the following manner (see ref 8): The Beer–Lambert Law for the absorption by the bead is $I = I_0 \times 10^{-A}$; where I is the intensity at a specific point within the bead, I_0 is the incident intensity; $A = \epsilon cl$ (assuming an $\epsilon =$ extinction coefficient; $20\,000 \text{ cm}^{-1} \text{ M}^{-1}$; c is the concentration within the bead, assuming 150 pmol of sites/bead, $100\text{-}\mu\text{m}$ diameter, and concentration of 0.3 M ; l is the path length into the bead; and $50 \mu\text{m} = 50 \times 10^{-4} \text{ cm}$). Thus, at the center of the bead, $A = 30$ ($A = \epsilon cl$, $20\,000 \text{ M}^{-1} \text{ cm}^{-1} \times 0.3 \text{ M} \times 50 \times 10^{-4} \text{ cm}$), and there can be NO illumination ($I = I_0 \times 10^{-30}$!!). At $1 \mu\text{m}$ depth, $A = 0.6$; at $10 \mu\text{m}$, $A = 6$). This situation will improve only if only a fraction of the sites are loaded (i.e., reducing the concentration on the bead). Thus, the reduction in intensity caused by absorption of the dyed bead is given by $I = I_0 \times 10^{-Af}$ ($f =$ filling factor). For occupancies above $f = 10^{-2}$ (i.e., $>1\%$ loading), the bead will be optically thick, and the exponential will depart

* To whom correspondence should be addressed. E-mail: mb14@oton.ac.uk.

[†] Department of Chemistry, University of Southampton.

[‡] Department of Physics and the Opto-Electronics Research Centre, University of Southampton.

[§] GlaxoSmithKline, Chemistry Technologies, Department of Chemistry, University of Cambridge.

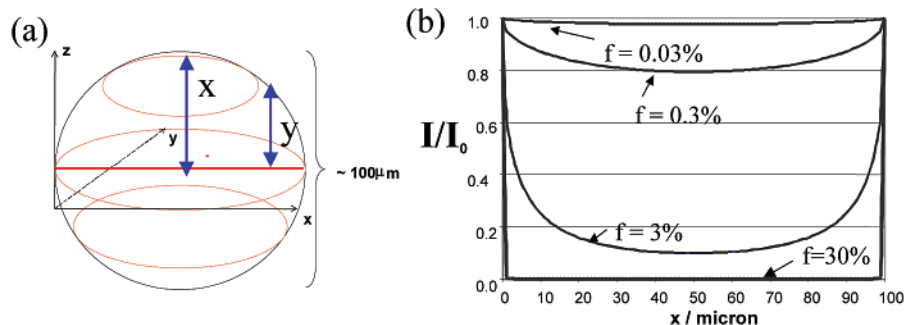


Figure 1. (a) Representation of a resin bead. The dot within the bead correlates to the volume element of a single scan. About 170 000 spectra are possible for a 100- μm bead! The interrogation distance to the center of the bead (x) is much greater than at the edge (y). (b) Penetration of light to the equatorial plane of the bead as a function of absorbance, assuming an extinction coefficient of $20\,000\text{ cm}^{-1}\text{ M}^{-1}$ and a concentration within the bead when fully loaded (assuming 150 pmol of sites/bead, 100 μm diameter) of 0.3 M and various occupancies (f) ranging from 30% (0.1 M) to 0.03% (100 μM).

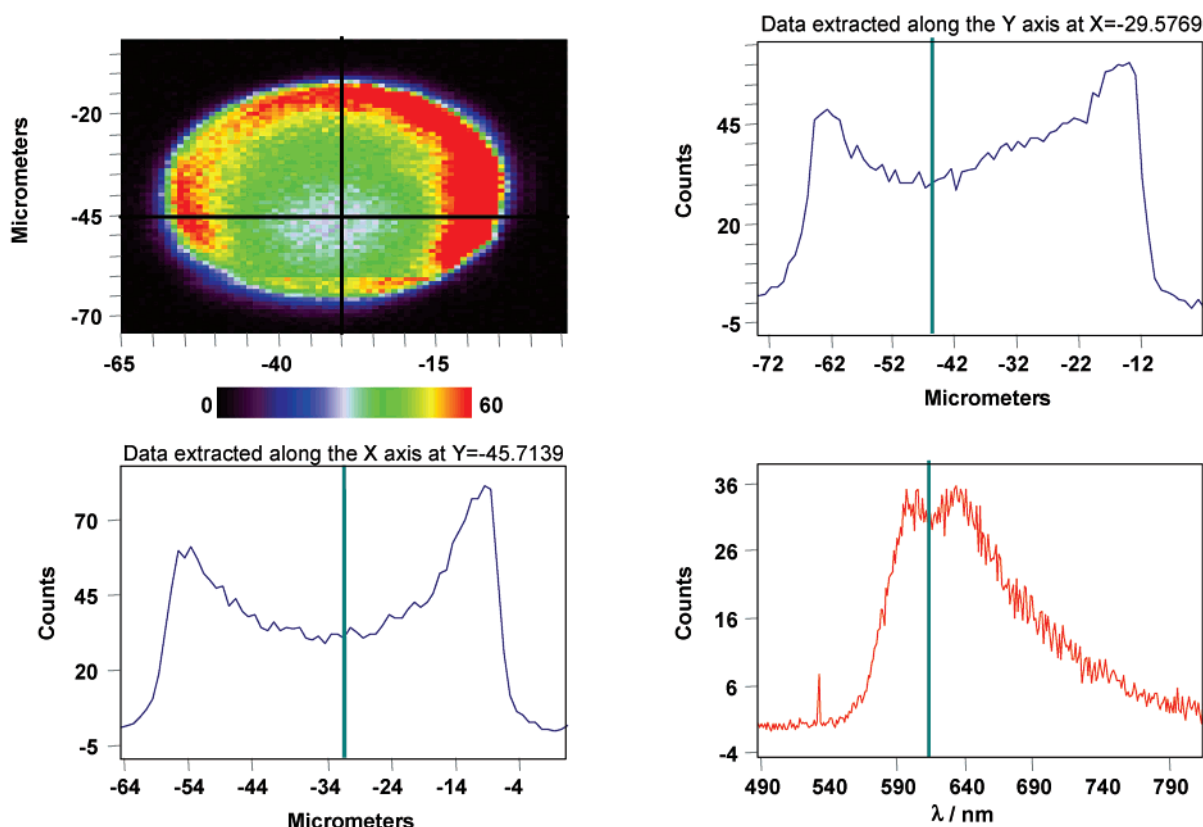


Figure 2. “Apparent” nonuniform distribution of reacted sites on a loaded PS bead.

significantly from a linear relationship between dye loading and fluorescent intensity.

Thus, spectra such as those shown in Figure 2 would wrongly suggest a higher number of functional groups at the surface of the bead but are merely artifacts due to working at too high a fluorophore loading (as discussed above).

Another significant issue with fluorescent measurements is one of dye bleaching. This problem is illustrated in Figure 3, which shows the decrease in fluorescence intensity obtained from sequential measurements on the same PEGA resin bead (loaded $\sim 1\%$ with RITC, swollen in water). It is clear that the dye is being destroyed by the laser radiation under these conditions; however, the extent of bleaching is very material- and solvent-dependent. On PEGA and Tenta-Gel resins, bleaching was a significant problem, but on glass and PS, similar laser powers resulted in little or no bleaching.

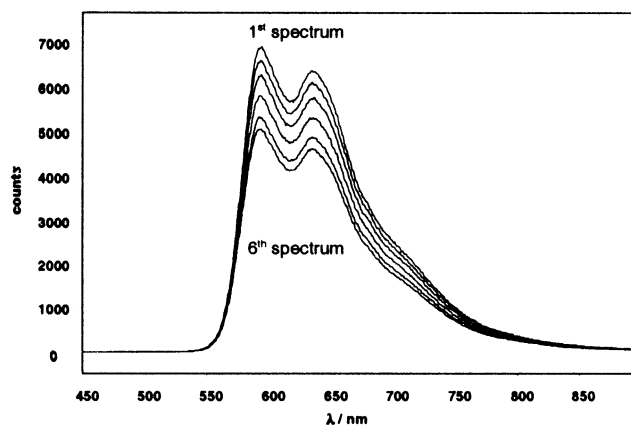


Figure 3. Bleaching of the rhodamine dye on PEGA resin (1% loading, bead swollen in water, scanning every 5 s).

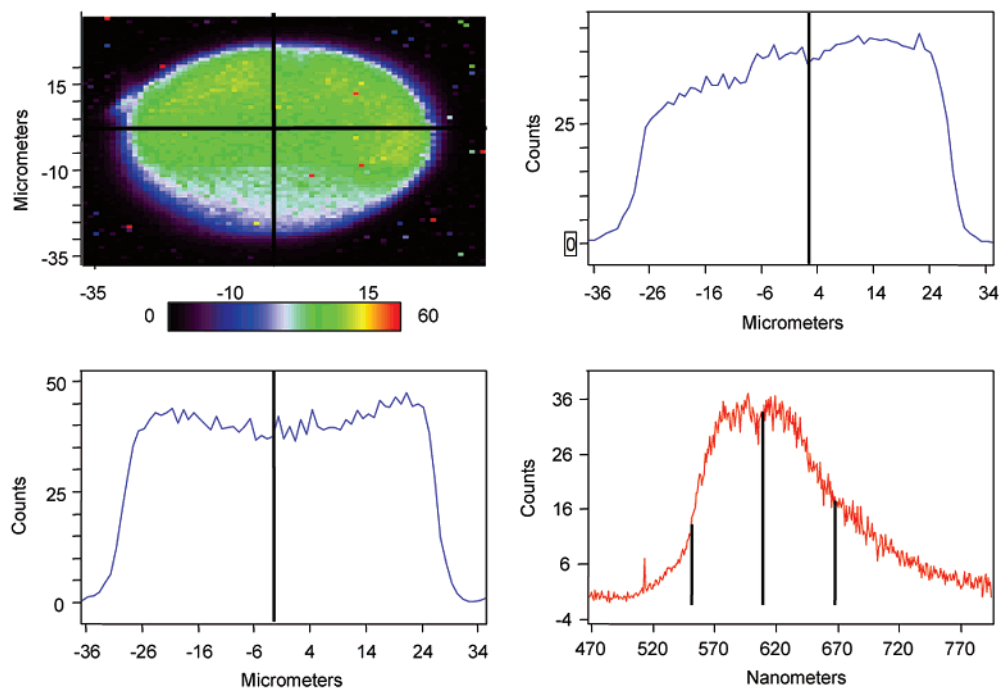


Figure 4. Map of fluorescence on a glass bead (bead loading $\sim 1\%$ with rhodamine) showing the uniform site distribution.

The rationale for this is unclear, although we propose it may relate to the increased mobility of the fluorophores on the PEG based resins.

Thus, if the loading is carefully chosen, the laser power is reduced, and reabsorption problems and bleaching of the rhodamine can be excluded, then this method can be used to screen bead functionality. Figure 4 shows one example of a glass bead treated with 1% RITC showing the relative intensity of the fluorescence spectra recorded along the crosshair in the x and y directions. There is no significantly higher intensity at the edge of the bead.

A similar picture was observed for all the other materials investigated with both dry and swollen beads at very low loadings. Therefore, it can be concluded that the functional site distributions in PS, TG, PEGA, and CPG are uniform.

However, these studies do demonstrate that there are serious issues relating to absorbance when fluorescence studies are carried out on resin beads. This is especially important if reaction kinetics and site profiles are to be determined on beads in a manner that requires high bead loadings. We, therefore, turned to another method of bead investigation that does not suffer from these limitations. Confocal Raman microscopy allows Raman spectra to be recorded from a volume element of $\sim 1 \times 1 \times 3 \mu\text{m}^{11,12}$ from anywhere within the bead with a spectral resolution 0.1 cm^{-1} . Raman excitation was performed at a wavelength well-removed from the absorption bands of the supports and to the long wavelength side of the absorption band. In this situation, with a relatively small Raman shift (vibrational band), the shift takes it to longer wavelengths further away from the absorption band, and therefore, the illumination intensity will be uniform throughout the bead. The intensity of the Raman peak is, therefore, proportional to the number of Raman active groups present in the confocal volume regardless of the location of this volume within the bead (center, surface, edge). Therefore, confocal Raman spectroscopy

avoids some of the complexities of fluorescence spectroscopy highlighted above. Spectra can be collected in a consecutive fashion, for example, along a line within a bead or in a plane $3 \mu\text{m}$ thick (a slice)¹¹ either after quenching the reaction or by imaging the whole bead in real time, thus allowing whole-bead reaction kinetics to be obtained. Raman spectroscopy thus provides a very useful probe of the spatial and temporal distribution of reactive sites within a polymer bead. In addition, Raman spectra are sensitive to the nature of the environment around these sites, and this can be used to extract information concerning the bead environment that is impossible to obtain in other ways.

To investigate whole bead reaction kinetics, 4-cyanobenzoic acid (4-CBA) was loaded onto aminomethyl functionalized solid supports (TentaGel and PS) in dioxane with 1,3-diisopropylcarbodiimide (DIC) as the coupling reagent. The concentration of the components in the mixture was chosen to be low (16 mM), which made it possible to quench the reaction prior to completion. Figure 5 shows the relative intensity of the CN stretching frequency in the Raman spectrum of a whole bead, which was taken out from the reaction mixture and clearly shows second-order reaction kinetics under these conditions. Using these beads and scanning in a confocal mode, it was possible to determine which sites on the resin beads were reacting first. Thus, resin beads were analyzed by accumulating a line scan across the bead through the equatorial plane at several different reaction times. The results from a polystyrene resin bead are presented in Figure 5b and show a uniform distribution across the bead. With time loading increases, again with a uniform distribution, hence, indicating that in this case, the rate of coupling is slower than diffusion of the reagents into the bead.

However, with TentaGel resin in dioxane, the situation was remarkably different. Figure 6a,b shows the data obtained from a partially loaded TentaGel resin bead. The CN-Raman signal was recorded at 2800 individual points

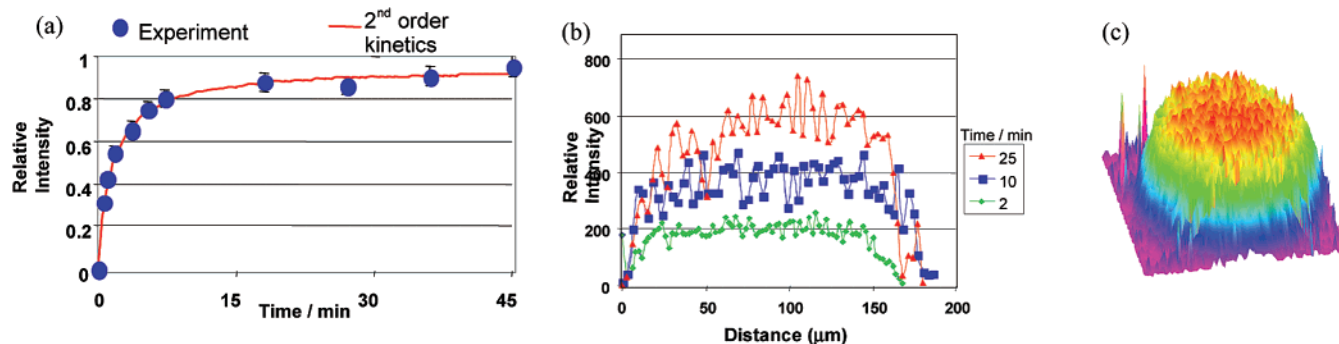


Figure 5. (a) Reaction kinetics on PS beads. Relative intensity of the CN Raman signal of a reaction run with 16 mM 4-cyanobenzoic acid/DIC in dioxane. Beads were taken out from the reaction mixture, washed, and analyzed. (b) Intensity of the CN Raman signal taken as a line scan across the PS bead. (c) 3D-pictorial representation of site functionalization.

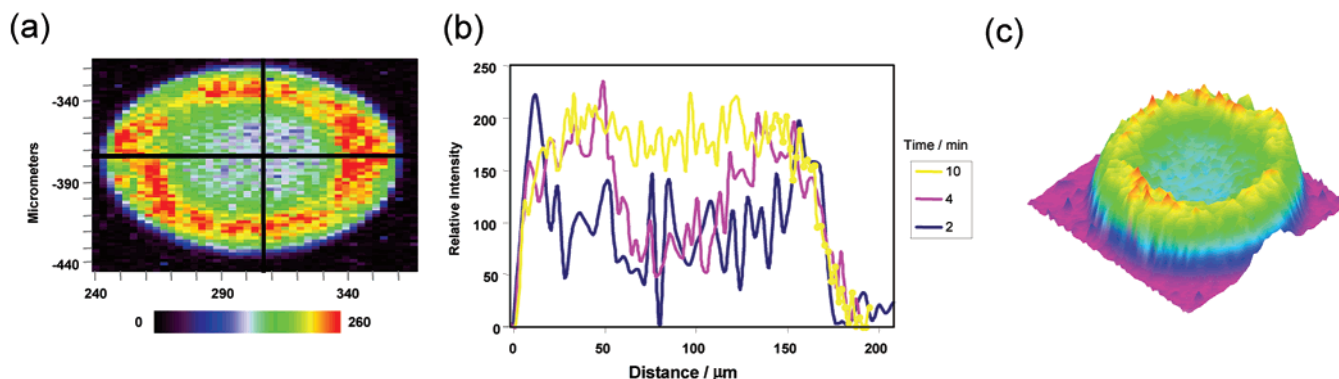


Figure 6. (a) Site distribution on a partially loaded TentaGel resin bead (4-CBA/DIC (16 mM) in dioxane). (b). Reaction profile across the TentaGel Resin bead with time; the “hole” in the center fills. (c) 3D-pictorial representation of site functionalization after 2 min.

within an equatorial plane, and the relative intensity was assigned to a color code. The “doughnut” band of intensity clearly illustrates that not all sites on the resin bead react at the same rate and that the reaction between 4-cyanobenzoic acid and the aminomethyl groups of TentaGel-resin is diffusion controlled. Thus, the outer region of the bead is loaded preferentially in this case. After sufficient reaction time, the loading profile becomes uniform across the bead. This is exemplified in Figure 6b, which illustrates that although the outside reacts “faster”, the whole bead will with time become fully loaded.

Fluorescence microscopy is a powerful technique for analyzing beads with very low loading of fluorophores. However, a major issue is that fluorescence is fundamentally flawed when looking at highly loaded beads. At higher loadings, fluorescence dyes bring problems mainly due to absorption, but also dye–dye interactions, spectral shifts, and quenching, rendering this highly sensitive technique much less useful. Without considerable care in the design of the experiment, the observed distributions will be distorted from the true distribution within the bead. To probe the distributions at higher loading fractions, Raman spectroscopy avoids many of the problems associated with fluorescence studies. The ability to use an excitation wavelength removed from any absorption features reduces the problems associated with nonuniform excitation across the bead, while the relative insensitivity of the vibrational lines to the environment reduces the problem of interactions between the probe species. This weakness of the Raman technique means it is suitable for the investigation of more heavily loaded beads.

Our studies using these techniques thus show that there is a uniform distribution of reactive sites throughout the beads but that the spatial distribution of reacted sites depends on the polymer type, with a fine balance between reaction and diffusion rate. On PS resin beads, there was, in this case, a uniform distribution of sites, with the reaction rate being slower than diffusion. However, on TentaGel, this was not the case. Here, the reaction between 4-cyanobenzoic acid and the aminomethyl groups of the TentaGel-resin was diffusion-controlled.

Experimental Details

Since the source of the solid supports might be an important issue in this context, the exact specification of the beads used in this work is given: TG, Advanced ChemTech Catalogue no. SJ6009, batch 15695, bead diameter 130 μm , 1% cross-linked with divinyl benzene (DVB); Amino PEGA, NovaBiochem Catalogue no. 01-64-0100, batch A18351; Aminomethylated PS, NovaBiochem Catalogue no. 01-64-0010, batch A21162, bead diameter 75–150 μm ; CPG Amino 155, Johns Manville Sales GmbH Germany Catalogue no. L 05/95, bead diameter 100–200 μm , pore size 100 nm. The beads were swollen in DMF and reacted with RITC corresponding to 1% of the loading given by the supplier. The reaction mixture was shaken overnight, and the beads were washed with DMF, MeOH, and DCM and were dried in vacuo. The fluorescence spectra were recorded using a Renishaw 2000 system set to the confocal mode, irradiation with an Ar-ion laser (488 nm), 900 Groove grating. Raman spectra were recorded using a Renishaw 2000 system, set to

the confocal mode, irradiation with a HeNe laser (633 nm), and a 1800 Groove grating. The maps were created using the mapping program supplied with the WIRE (Windows-based Raman Environment) program from Renishaw. The identification of 4-nitrile benzamide attached to the resin was proven by attachment of a Rink linker and subsequent cleavage and analysis of the product 4-nitrile-benzamide. Data for 4-cyanobenzamide: δ_{H} (300 MHz, d_6 -DMSO) 7.70 (1H, s, NH), 7.98 (4H, AB system, ArH), 8.22 (1H, s, NH); δ_{C} (75 MHz, d_6 -DMSO) 113.7 and 118.5 (NC- and NC-C), 128.3 (ArC-3,5), 132.5 (ArC-2,6), 166.5 (CONH₂); m/z (ES + ve) (M + H⁺)⁺ 147 (100%).

Acknowledgment. ESPRC/GSK for a Combinatorial Chemistry Project Grant

References and Notes

- (1) Dörwald, F. Z. *Organic Synthesis on Solid Phase*; Wiley-VCH: Weinheim, 2000. Seneci, P. *Solid-Phase Synthesis and Combinatorial Technologies*; Wiley-VCH: Weinheim, 2000. Guillier, F.; Orain, D.; Bradley, M. *Chem. Rev.* **2000**, *100*, 2091. Arya, P.; Chou, D. T. H.; Baeck, M.-G. *Angew. Chem., Int. Ed.* **2001**, *40*, 339. Ley, S. V.; Baxendale, I. R.; Bream, R. N.; Jackson, P. S.; Leach, A. G.; Lonbottom, D. A.; Nesi, M.; Scott, J. S.; Storer, R. I.; Taylor, S. J. *J. Chem. Soc., Perkin Trans. 1* **2000**, 3815. Kirschning, A.; Monenschein, H.; Wittenberg, R. *Angew. Chem., Int. Ed.* **2001**, *40*, 650. Vos, D. E. D., Vankelcom, I. F. J., Jakobs, P. A., Eds. *Chiral Catalyst Immobilization and Recycling*; Wiley-VCH: Weinheim, 2000.
- (2) Bosworth, N.; Towers, P. *Nature* **1989**, *341*, 167.
- (3) Michael, K. L.; Taylor, L. C.; Schultz, S. L.; Walt, D. R. *Anal. Chem.* **1998**, *70*, 1242. Dickinson, T. A.; White, J.; Kauer, J. S.; Walt, D. R. *Nature* **1996**, *382*, 697.
- (4) For example, the AlphaScreen technology of Packard which utilizes a bead-based, proximity-based homogeneous assay.
- (5) Sarin, V. K.; Kent, S. B. H.; Merrifield, R. B. *J. Am. Chem. Soc.* **1980**, *102*, 5463.
- (6) Roscoe, S. B.; Frechet, J. M. J.; Walzer, J. F.; Dias, A. J. *Science* **1998**, *280*, 270.
- (7) (a) Kress, J.; Rose, A.; Frey, J. G.; Brocklesby, W. S.; Ladlow, M.; Mellor, G. W.; Bradley, M. *Chem. Eur. J.* **2001**, *7*, 3880. (b) Rademann, J.; Barth, M.; Engelhaaf, H.-J.; Jung, G. *Chem. Eur. J.* **2001**, *7*, 3884.
- (8) Egner, B. J.; Rana, S.; Smith, H.; Bouloc, N.; Frey, J. G.; Brocklesby, W. S.; Bradley, M. *Chem. Commun.* **1997**, 735.
- (9) Scott, R. H.; Balasubramanian, S. *Bioorg. Medchem. Lett.* **1997**, *7*, 1567. Yan, B.; Martin, P. C.; Lee, J. J. *Comb. Chem.* **1999**, *1*, 78.
- (10) McAlpine, S. R.; Schreiber, S. L. *Chem. Eur. J.* **1999**, *5*, 3528.
- (11) There has been considerable discussion recently in the literature over the depth resolution than can be expected from a confocal microscope when it is used to probe relatively deeply inside a material. Everall (Everall, N. J. *Appl. Spectrosc.* **2000**, *54*, 773) pointed out that the presence of the air/sample interface (in our case, the air/solvent interface for the swollen beads) adversely affects the confocal properties and would lead to a very much worse depth resolution than would occur in air. Subsequent extension of this analysis (Baldwin K. J.; Batchelder, D. N. *Appl. Spectrosc.* **2001**, *55*, 517) modified these conclusions, showing the situation was not quite as problematic. However, these analyses do not correspond exactly to our observation conditions. To assess the actual depth resolution in our experiments, we recorded scans both across and down through a swollen spherical bead. A comparison of these two scans indicates a depth resolution of between 10 and 15 μm .
- (12) Most of our observations have been made on swollen beads. Typically, the polymer beads swell to twice their diameter in the solvent, and thus, on the order of 7/8 of the bead is now solvent. This automatically ensures that the bead is index-matched with the surrounding solvent (indeed, the swollen beads can be hard to see under the microscope). This removes the refractive focusing effect of the spherical bead surface. In the case of the dry beads, the refraction at the spherical surface bends the focal plane of the microscope considerably as the apparent position is probed away from the center line of the bead, making the interpretation of the observed spatial distribution in a dry bead harder to interpret than in the much more straightforward situation of the swollen beads.

CC020024X